Inorganic Chemistry

Article

pubs.acs.org/IC

Synthesis of Zwitterionic Triphosphenium Transition Metal Complexes: A Boron Atom Makes The Difference

Jonathan W. Dube,[†] Charles L. B. Macdonald,[‡] Bobby D. Ellis,[§] and Paul J. Ragogna*[,†]

[†]Department of Chemistry and The Center For Advanced Materials and Biomaterials Research (CAMBR), The University of Western Ontario, 1151 Richmond Street, London, Ontario N6A 5B7, Canada

[‡]Department of Chemistry and Biochemistry, The University of Windsor, 401 Sunset Avenue, Windsor, Ontario N9B 3P4, Canada

[§]Department of Chemistry, Acadia University, 6 University Avenue, Wolfville, Nova Scotia B4P 2R5, Canada

Supporting Information

ABSTRACT: A collection of zwitterionic phosphanide metal carbonyl coordination complexes has been synthesized and fully characterized, representing the first isolated series of metal complexes for the triphosphenium family of compounds. The dicoordinate phosphorus atom of the zwitterion is formally in the +1 oxidation state and can coordinate to one metal, **2M** (M = Cr, Mo, W) and **2Fe**, or two metals, a $Co_2(CO)_6$ fragment **4**, depending on the starting reagents. All complexes have been isolated in greater than 80% yield, and structures were confirmed crystallographically. Metrical parameters are consistent with **1** being a weak donor and results in long metal−phosphorus bonds being observed in all cases. Unique bimetallic structures, **3M** (M = Cr, Mo, W), consisting of a $M(CO)_5$ fragment on phosphorus and a piano-stool $M(CO)_3$ fragment on a boron phenyl group have been identified in the $^{31}P\{^1H\}$ NMR spectra and confirmed using X-ray diffraction studies. Use of the borate backbone in **1**, which renders the molecule zwitterionic, proves to be a determining factor in whether these metal complexes will form; the halide salt of a cationic triphosphenium ion, **6**[Br], shows no evidence for formation of the analogous metal complexes by $^{31}P\{^1H\}$ NMR spectroscopy, and tetraphenylborate salts, **6**[BPh_4] and **7**[BPh_4], produce complexes that are unstable.

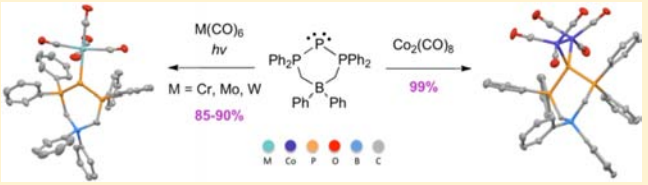

INTRODUCTION

Although the use of *N*-heterocyclic carbene (NHC) ligands continues to expand throughout organometallic chemistry, organophosphines remain the most ubiquitous ligand class due to their commercial availability and ease for synthetic modification. Trivalent phosphorus compounds, phosphines, are common two-electron donors that adopt a traditional donor → acceptor bonding motif when paired with transition metals or Lewis acids. Compounds with univalent phosphorus such as free phosphinidenes, **A**, are far less prevalent in the literature due to their electron deficiency, significantly heightened reactivity, and propensity to oligomerize under ambient conditions (i.e., $(PhP)_5$ **B**), Figure 1.[1−3] Such oligomerization of the putative, triplet, phosphinidene fragments fills all of the vacant orbitals and results in considerably more stable species. There are however chemical modifications that can be made to stabilize phosphorus(I) centers and render them useful in onward transformations. For example, phosphinidenes have a long history of being trapped in the coordination sphere of transition metals, **C**, typically by high-yielding salt elimination reactions.[4−6] These types of compounds can be considered electrophilic (Fischer type)[7] or nucleophilic (Schrock type)[8] and have been reviewed on a number of occasions.[9−11] The philicity and reactivity of the phosphinidene is strongly dependent on the ancillary ligands on the metal center; strong σ donors enhance the nucleophilicity at phosphorus (i.e., **D**), while strong π acceptors increase the electrophilicity at phosphorus (i.e., **E**).[12] Two recent highlights for the metal P(I) systems include deoxygenation of carbon dioxide reported by Streubel[13] and activation of H_2 reported by Mathey.[14] In both cases the phosphinidene resembles compound **E** and is thermally generated in situ from a stable P(III) source, which then goes on to react with the given substrate. Metal-free systems can be observed using a strong sigma donor like an NHC to break apart the $(PhP)_5$ pentamer and form the stable and isolable base-stabilized phosphinidene complex (**F**). The electron-rich nature of the phosphorus atom is confirmed by its ability to coordinate to two BH_3 molecules concurrently (**G**).[15] Alcarazo et al. utilized the strongly donating cyclopropylidene NHC to isolate a P(I) adduct that can then coordinate to either two {AuCl} fragments or one {AuCl} and one {Rh(COD)Cl} fragment simultaneously (**H**).[16] This recent report highlights the first use of both lone pairs of electrons on phosphinidenes to coordinate to two different metal centers at the same time. A broader application of these types of molecules exists using $^{31}P\{^1H\}$ NMR spectroscopy as a sensitive probe on the electronic environment of the phosphorus atom to determine the relative π-acceptor ability of NHC's.[17] A structurally similar base-stabilized phosphinidene complex, formally a phosphanylidene phosphorane, with PMe_3 in place of the NHC (**I**) was

Received: July 9, 2013
Published: September 18, 2013

   dx.doi.org/10.1021/ic401766j | *Inorg. Chem.* 2013, 52, 11438−11449

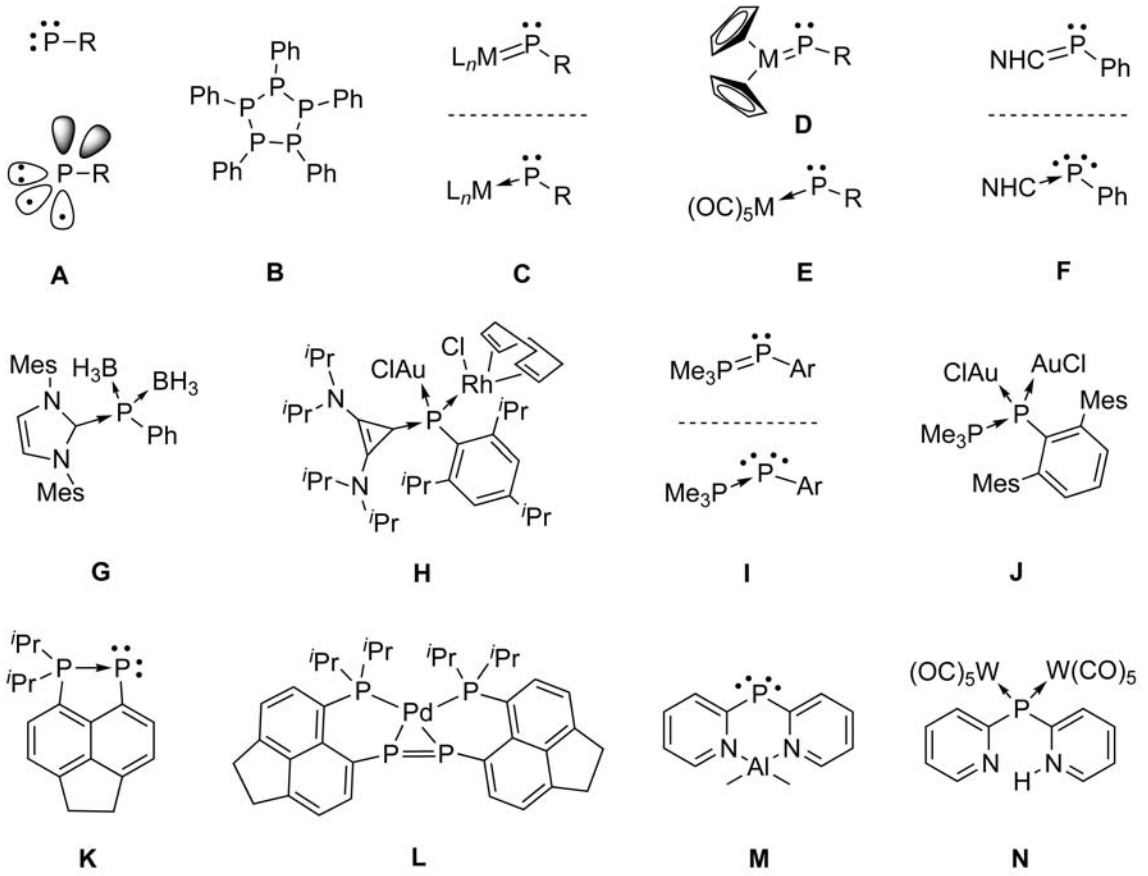

Figure 1. Structural representations of phosphorus(I) systems, and some examples of their corresponding metal complexes. Note that Mes = 2,4,6-trimethylphenyl.

synthesized by Protasiewicz et al.,[18] which can then coordinate to two {AuCl} fragments at the same time (**J**).[19] Adopting the same bonding motif into a rigid cyclic *peri*-acenaphthene system results in a sterically accessible P(I) center (**K**) that can then coordinate to two BH_3 molecules or form a novel 2:1 Pd(0) complex (**L**).[20] Stalke and co-workers prepared a unique metallophosphane (**M**) which has been shown to possess two lone pairs of electrons on the phosphorus atom by charge density studies as well as coordination to two $\{W(CO)_5\}$ fragments (**N**) or to manganese and cesium.[21−24] While the above examples are key breakthroughs in the coordination chemistry of low oxidation state phosphorus, they are often not general, and examples of cationic or neutral P(I) systems bonding to different transition metals remain rare.

Triphosphenium ions (**O**) are an established class of P(I) compounds first developed by Schmidpeter (Figure 2) that have received almost no attention as a ligand for transition metals.[25−30] This is despite theoretical investigations confirming that the electron-rich phosphinidene or phosphanide bonding model is most appropriate for these compounds.[31,32] The dearth of coordination chemistry probably results from several factors: (1) the presence of a positive charge on the ligand framework, which lowers the energies of the frontier orbitals rendering the "lone pairs" of electrons less accessible, (2) the accompanying anion, typically $[AlCl_4]^-$ or $[SnCl_5]^-$, is potentially reactive and can interfere with onward transformations, and (3) significant π-back-bonding from the low-coordinate P(I) center to the flanking phosphines further lowers/stabilizes the HOMO energy. Strong evidence for the

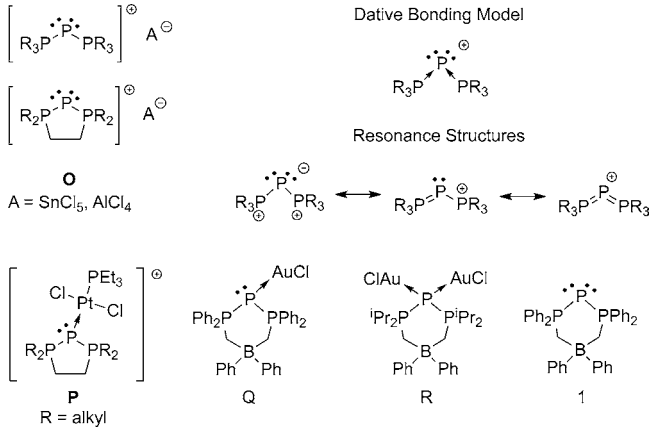

Figure 2. Structural representations of triphosphenium ions and the first isolated coordination compounds utilizing a zwitterionic system.

synthesis of triphosphenium−platinum complexes (i.e., **P**) was compiled by Dillon et al.; however, no structural verification was obtained.[33] Previously, we demonstrated that incorporating a borate anion into the ligand backbone and rendering the molecule zwitterionic increases the electron density at phosphorus and thus allows the "lone pairs" of electrons to be more accessible for coordination to transition metals. This subtle modification in ligand design provided the first isolable coordination compounds of a triphosphenium ion, which proved capable of binding to one or two {AuCl} fragments simultaneously depending on the substituents on the

dx.doi.org/10.1021/ic401766j | *Inorg. Chem.* 2013, 52, 11438−11449

phosphorus atoms (**Q**, **R**; Figure 2).[34] Compound **R** is the first experimental evidence for triphosphenium complexes to have phosphinidene character, where both "lone pairs" of electrons on phosphorus are utilized simultaneously, analogous to the neutral base-stabilized compounds previously discussed.

In order to expand on the coordination chemistry of the unique zwitterionic system we treated the parent P(I) proligand (**1**) with a variety of metal carbonyl starting materials. In this context, reaction of either $M(CO)_6$ (M = Cr, Mo, W) or $Fe(CO)_5$ with **1** in the presence of UV light results in formation of traditional metal complexes **2M** and **2Fe**. Longer radiation times with excess metal carbonyl results in partial functionalization of a phenyl group on boron, **3M** instead of further coordination to another $M(CO)_5$ fragment through phosphorus. Compound **1** is shown to act as a novel 4 electron μ-type donor to a $\{Co_2(CO)_6\}$ fragment, **4**, which is isolated from reaction of **1** with $Co_2(CO)_8$. In all cases the metrical parameters are consistent with **1** being a weak donor, while the P–W coupling constant in **2W** supports this observation. These results represent a series of unique P(I) coordination compounds, all synthesized in excellent yields as crystalline solids and fully characterized, where analogous complexes cannot be isolated from the cationic triphosphenium ions.

RESULTS AND DISCUSSION

The 1:3 stoichiometric reaction of the phosphorus(I) proligand (**1**) and a group 6 metal carbonyl, $M(CO)_6$ (M = Cr, Mo, W), in THF under UV light for 24 h gives rise to a bright yellow solution (Scheme 1, top). The crude reaction mixture can be

Scheme 1. Synthesis of the $M(CO)_5$ Coordination Complexes, 2M (M = Cr, Mo, W), and $Fe(CO)_4$ Coordination Complex 2Fe (top) and the Conditions Required for Observation of the Bimetallic Minor Product, 3M, (M = Cr, Mo, W) (bottom)

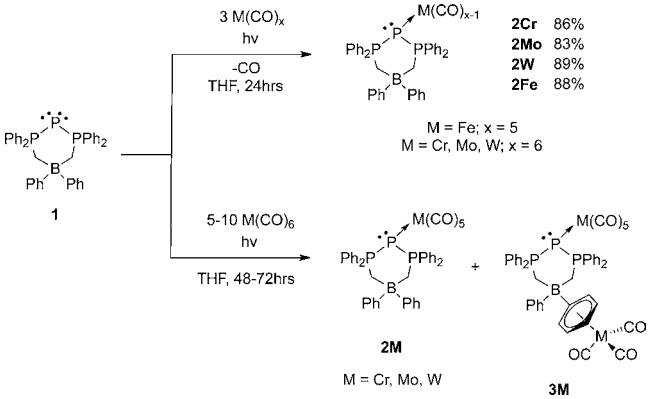

easily monitored using $^{31}P\{^1H\}$ NMR spectroscopy to determine when the reaction is complete. Crude powder was isolated after removal of all volatile components; this was then dissolved in Et_2O, filtered, and concentrated in vacuo to give a yellow solid. Analysis of the isolated solids by $^{31}P\{^1H\}$ NMR spectroscopy in $CDCl_3$ reveals the triplet shifted considerably downfield (δ_P = −116, −139, and −152 for Cr, Mo, and W, respectively) from the parent ligand (cf. δ_P = −221 in $CDCl_3$) consistent with binding to an electrophilic metal center (Figure 3). There is also a corresponding decrease in the phosphorus–phosphorus one-bond coupling constants ($^1J_{P-P}$ = 364, 350, and 345 Hz for Cr, Mo, and W, respectively; cf. 414 Hz for **1**) consistent with a decrease in the P–P bond order. The doublet resonance attributable to the flanking phosphorus atoms also shifts downfield (δ_P = 40, 38, and 36 for Cr, Mo, and W, respectively; cf. 34 for **1**), which differs from the corresponding, previously reported,[35] arsenic complexes; in this case the resonance for Mo and W complexes is upfield compared to the free ligand. The tungsten derivative also clearly shows the presence of ^{183}W satellites ($^1J_{^{183}W-P}$ = 134 Hz), with the coupling constant being considerably smaller than that observed for more typical phosphine–$W(CO)_5$ coordination complexes (cf. $^1J_{^{183}W-P}$ = 280 Hz for $Ph_3P{\rightarrow}W(CO)_5$).[36] ^1H NMR spectra of all group 6 derivatives reveal a symmetrical ligand environment in solution with a slight downfield shift in the methylene protons (δ_H = 2.28, 2.26, and 2.29 for Cr, Mo, and W, respectively, cf. 2.18 for **1**). Analysis of the purified solids by FT-IR spectroscopy reveals the typical ligand stretches in addition to four intense signals between 1800 and 2100 cm^{-1}, consistent with the presence of a $\{M(CO)_5\}$ fragment in an asymmetrical environment in the solid state. Single crystals suitable for X-ray diffraction experiments were obtained from saturated Et_2O solutions at −35 °C and confirmed the structures to be the expected metal coordination complexes, **2M** (M = Cr, Mo, W), which were all isolated in greater than 80% yield. Reaction of **1** and two stoichiometric equivalents of $Fe(CO)_5$ proceeds in an analogous manner to those of the group 6 carbonyls and produces a dark orange powder. Analysis of the product by $^{31}P\{^1H\}$ NMR spectroscopy reveals the diagnostic signals (d, δ_P = 36; t, δ_P = −89; $^1J_{P-P}$ = 378) with the triplet being shifted further downfield than for **2M** (Figure 3). The ^1H NMR spectrum again reveals a symmetric ligand environment, while the FT-IR spectrum displays three CO stretches. The solid-state structure was confirmed to be the expected $Fe(CO)_4$ complex (**2Fe**), and the product was isolated in 89% yield. The zwitterionic nature of these complexes renders them highly soluble in polar (i.e., CH_2Cl_2, THF) and nonpolar solvents (i.e., Et_2O, toluene) alike. Some decomposition back to the free ligand (ca. 5%) is observed in chlorinated solvents after approximately 24 h, but the materials appear to be indefinitely stable in the solid state under a nitrogen atmosphere at room temperature.

The trend of increasing shielding observed for the chemical shift of the triplet signal in the series of mononuclear complexes **2Fe**, **2Cr**, **2Mo**, and **2W** illustrated in Figure 3 is clear. In an attempt to rationalize this trend, we performed a series of density functional theory (DFT) NMR calculations using simple models of the complexes in which all phenyl substituents are replaced with hydrogen atoms (**1**$^{\mathbf{H}}$, **2**$^{\mathbf{H}}$**Fe**, **2**$^{\mathbf{H}}$**Cr**, **2**$^{\mathbf{H}}$**Mo**, and **2**$^{\mathbf{H}}$**W**). The calculations reproduce the trend quite reasonably: the unique phosphorus atoms in all of the metal complexes are significantly deshielded with respect to that of the free ligand (**2**$^{\mathbf{H}}$), and the shielding of that nucleus in the complexes increases in the series Fe < Cr < Mo < W. As illustrated in Table 1, a more detailed analysis reveals that it is changes in the paramagnetic shielding (σ^p), as one would anticipate, that produce the observed trend, whereas the diamagnetic shielding (σ^d) terms are almost identical for the phosphorus atoms in all of the calculated model compounds. In general, the magnitude of σ^p is determined by the favorability of magnetic-dipole-allowed mixing of ground- and excited-state wave functions; σ^p is *deshielding* in nature for occupied virtual interactions. Moreover, because the HOMO in each of the complexes has a significant contribution from the unique phosphorus atom (attributable to the remaining "lone pair" of

dx.doi.org/10.1021/ic401766j | *Inorg. Chem.* 2013, 52, 11438–11449

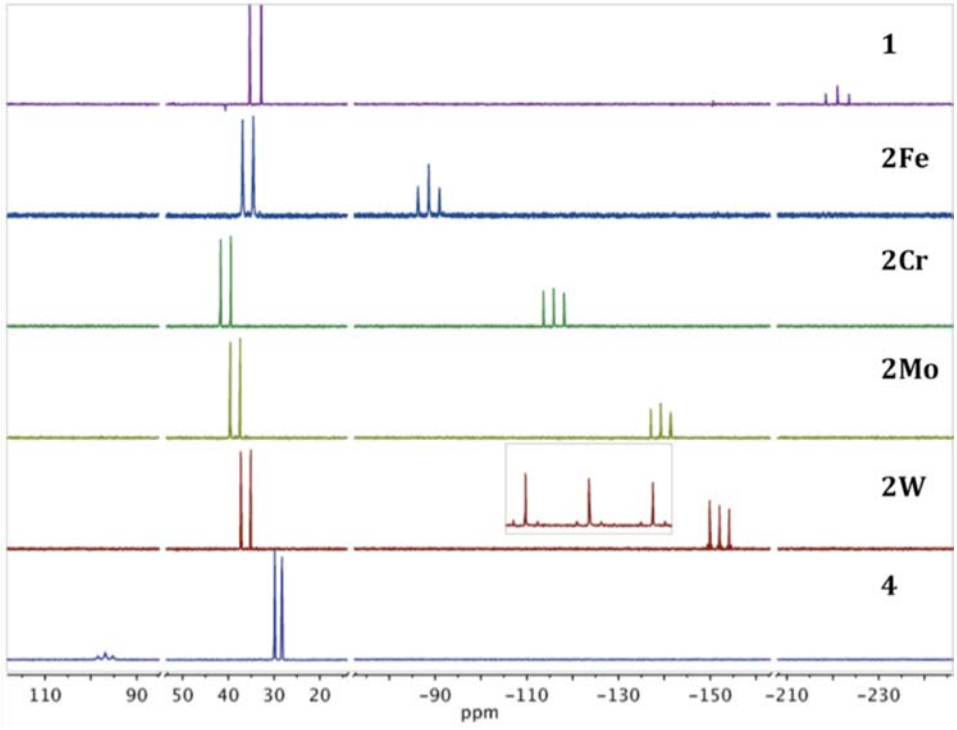

Figure 3. Stack plot of the $^{31}P\{^{1}H\}$ NMR spectra for **1**, **2Fe**, **2M** (M = Cr, Mo, W), and **4** from top to bottom. Inset for **2W** displays the satellite signals observed due to coupling to ^{183}W (14% abundant).

Table 1. Important Results of DFT Calculations of ^{31}P NMR Parameters for the Unique Phosphorus Atom in Relevant Geometry-Optimized Model Compounds

			isotropic shielding values (ppm)				
model	label	δ ^{31}P (ppm)	σ^{Total}	σ^{d}	σ^{p}	σ^{SO}	H−L (eV)
$[H_2PO_4]^-$		0	309.08	961.889	−667.487	14.682	
$P(H_2PCH_2)_2BH_2$	$\mathbf{1^H}$	−213.14	522.22	964.944	−457.599	14.880	3.579
LP−$Fe(CO)_4$	$\mathbf{2^HFe}$	−89.82	398.90	963.824	−590.229	25.307	2.399
LP−$Cr(CO)_5$	$\mathbf{2^HCr}$	−118.86	427.94	963.686	−556.086	20.341	2.718
LP−$Mo(CO)_5$	$\mathbf{2^HMo}$	−146.01	455.09	964.015	−533.710	24.781	2.797
LP−$W(CO)_5$	$\mathbf{2^HW}$	−154.92	464.00	964.546	−543.725	43.175	2.690

nonbonding electrons on P), the trend in the chemical shifts for the ligating phosphorus atoms correlates particularly well with the trend in HOMO−LUMO energy differences (H−L) within the complexes for the lighter transition metals. For the tungsten complex $\mathbf{2^HW}$, relativistic effects are particularly important, and it is the larger shielding attributable to spin−orbit coupling (σ^{SO}) that renders the ligating phosphorus atom more shielded than the one in the molybdenum analog.

Many attempts were made to synthesize the bimetallic species by reaction of **1** by varying the stoichiometric equivalents (5−10) of metal carbonyl (M = Cr, Mo) under UV radiation for greater than 48 h (Scheme 1, bottom). Compound **2M** was always observed as the major product by $^{31}P\{^{1}H\}$ NMR spectroscopy; however, in some cases a minor component (less than 10% by integration) with a very similar chemical shift and coupling constant to **2M** was also observed (Figures S21−S23, Supporting Information). Although this product could not be isolated and fully characterized, insight into its likely structure was obtained from a single-crystal X-ray diffraction study on crystals obtained from vapor diffusion of CH_2Cl_2 into hexanes. The solid-state structure was revealed to be bimetallic, although only one metal was bound to the P(I) center, as in **2M**, with the second metal fragment being bound to a phenyl group on boron in an η^6-type fashion, **3M** (M = Cr, Mo). Analogous reactivity is not observed using a large excess of $Fe(CO)_5$, and instead, decomposition products are observed in the $^{31}P\{^{1}H\}$ NMR spectrum.

In an attempt to access both lone pairs of electrons on the central phosphorus atom metal carbonyl reagents with metal−metal bonds were selected. Unfortunately no reaction was observed with **1** and $Mn_2(CO)_{10}$ or $Ru_3(CO)_{12}$ under standard, thermal, or photolytic conditions for extended reaction times. However, 1:1 stoichiometric addition of **1** to $Co_2(CO)_8$ in CH_2Cl_2 results in immediate production of a dark purple solution (Scheme 2). In contrast to reaction of **1** with other metal carbonyls this reaction proceeds quickly, in less than 10 min, and without the presence of UV light. Removal of the volatile components gives a dark burgundy powder, which

dx.doi.org/10.1021/ic401766j | *Inorg. Chem.* 2013, 52, 11438−11449

Scheme 2. Synthesis of the $Co_2(CO)_6$ Coordination Complex 4

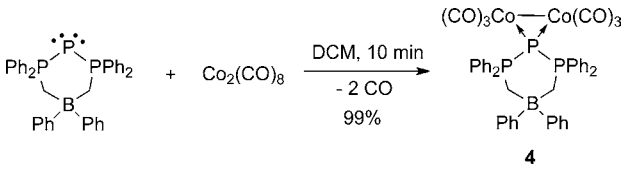

when redissolved in $CDCl_3$ reveals the characteristic doublet and triplet shifted slightly upfield and considerably downfield, respectively, in the $^{31}P\{^1H\}$ NMR spectrum (Figure 3; d, δ_P = 29; t, δ_P = 97). The corresponding coupling constant is also significantly lower than that for the free ligand and **2M** with a value of $^1J_{P-P}$ = 257 Hz. The FT-IR spectrum features four strong vibrations between 1900 and 2100 cm^{-1}, suggesting that there are no bridging CO ligands in the product. Analysis of single crystals produced from a Et_2O solution layered with pentane at −35 °C revealed the solid-state structure to be a $Co_2(CO)_6$ fragment bridged by **1** in μ_2 fashion (**4**). Beautiful confirmation for the presence of six CO ligands on cobalt comes from the ESI mass spectrum, where the parent ion is observed at 903 m/z ($[\mathbf{4} + Na^+]^+$) with good agreement to the calculated isotope pattern. From the parent ion, six consecutive signals are found 28 m/z units apart, consistent with successive loss of all six CO ligands from the molecule (Figure S29, Supporting Information). The product is isolated in quantitative yields and has similar solubility as the group 6 complexes.

Reaction of the related zwitterionic As(I) complex with group 6 carbonyls resulted in similar observations, data, and structures (Scheme 3).[35] However, reaction with $Co_2(CO)_8$ in 1:1 stoichiometry gives rise a new a signal in the $^{31}P\{^1H\}$ NMR spectrum (δ_P = 43), which is present in a 50:50 ratio to the starting material (δ_P = 31). Performing the reaction in a 1:2 ligand:metal stoichiometry results in complete conversion of the starting material to the new signal. Single-crystal diffraction studies on a dark red sample revealed the product to the bis(phosphino)borate-stabilized $Co(CO)_3$ complex, **5**, in which the low-coordinate arsenic atom has been displaced. There is no visible precipitate in the reaction mixture, so the fate of the arsenic atom is unknown, and a statement on the true outcome of the arsenic center is premature at this stage. A soluble cluster consisting of arsenic along with a number of cobalt carbonyl fragments is certainly possible. Evidence for such species is observed in the ESI-MS of the reaction mixture; however, X-ray-quality single crystals have presently not been isolated. There is precedence for this type of decomposition as complex arsenic clusters have been isolated from reaction of analogous cationic As(I) species with Me_3NO.[37] This result highlights the potential for drastic differences in reactivity between the zwitterionic phosphorus(I) and arsenic(I) systems.

Scheme 3. Previously Observed Coordination Chemistry with an As(I) Zwitterion (left), and the Observed Reactivity with $Co_2(CO)_8$ Resulting in Arsenic Displacement (right)

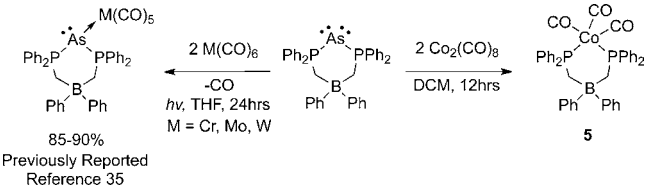

To evaluate whether our zwitterionic system is unique in acting readily as a ligand a comparison was carried out with the well-known cationic triphosphenium ions and the Lewis-acidic $\{M(CO)_5\}$ (M = Cr, Mo, W) fragments. The model cationic phosphorus compound chosen was [P(dppe)][Br] (**6**[Br]) because of its ease in synthesis and the fact that it is paired with the relatively unreactive anion compared to typical triphosphenium ions (cf. $AlCl_4$ and $SnCl_5$).[38] Reaction of **6**[Br] with three stoichiometric equivalents of $M(CO)_6$ under constant UV radiation for 48 h gives rise to a bright yellow solution (Scheme 4). The reaction mixture was regularly monitored by $^{31}P\{^1H\}$ NMR spectroscopy, which showed no indication of product formation (Figure S31, Supporting Information). It should be noted that the reaction was carried out in a 50:50 MeCN:THF mixture due to the significantly lower solubility of **6**[Br] when compared to **1** in THF. In the case of chromium there was visual evidence for decomposition, which was supported by $^{31}P\{^1H\}$ NMR spectroscopic data, whereas the molybdenum and tungsten cases show no reactivity spectroscopically with the generated $\{M(CO)_5\}$ fragment. Reaction of **6**[Br] and excess $Fe(CO)_5$ also results in no observed product formation under analogous conditions. The solvent media raises the possibility of MeCN competing with the triphosphenium ion for metal ion

Scheme 4. Attempted Synthesis of $M(CO)_5$ (M = Cr, Mo, W) or $Fe(CO)_4$ Adducts with Cationic Triphosphenium Ions[a]

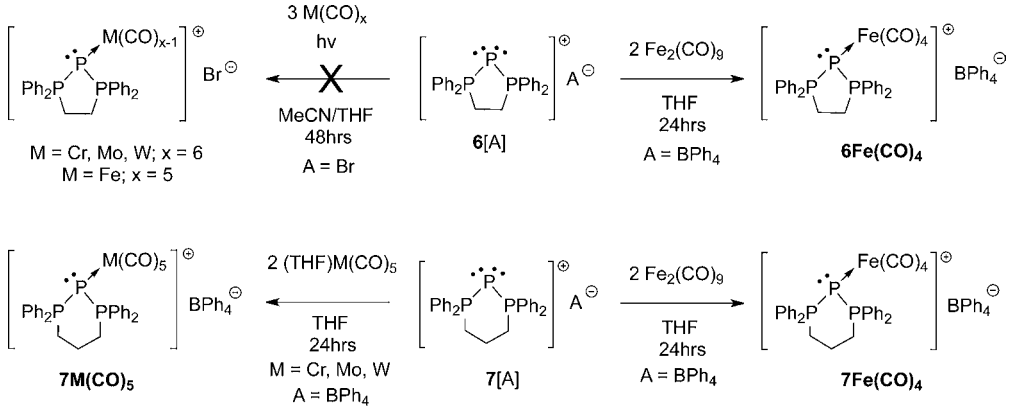

[a]With **6**[Br] no reaction is observed, while with **6**[BPh_4] or **7**[BPh_4] metal complexes are observed but the reaction does not go to completion and the products are not stable in solution. $^{31}P\{^1H\}$ NMR shifts for the observed products are listed in Table 2.

dx.doi.org/10.1021/ic401766j | Inorg. Chem. 2013, 52, 11438−11449

coordination but is a necessary consequence due to the solubility of **6**[Br]. This potential complication brings to light another advantage for the zwitterionic triphosphenium system, **1**, which is highly soluble in a range of organic solvents.

The apparent nonreactivity of the bromide salt **6**[Br] might be a consequence of the relative basicity of bromide anion; formation of salts of the type **6**[BrM(CO)$_5$] in solution would not be revealed by $^{31}P\{^1H\}$ NMR spectroscopy.[39] We note this possibility because, as indicated by the $^{31}P\{^1H\}$ NMR data in Table 2, treatment of **6**[BPh_4] or [P(dppp)][BPh_4], **7**[BPh_4], with $Fe_2(CO)_9$ does indeed generate iron tetracarbonyl complexes of triphosphenium cations. Similarly, reaction of (THF)M(CO)$_5$ solutions with **7**[BPh_4] produces the anticipated group 6 pentacarbonyl complexes (Scheme 4). However, it must be emphasized that, in contrast to the zwitterionic complexes described above, none of the reactions with cationic triphosphenium ions proceed to completion and the solids obtained upon removal of the volatile components are mixtures that include significant amounts of starting materials (see Figures S32–36, Supporting Information, for $^{31}P\{^1H\}$ NMR spectra of the Fe, Cr, Mo, and W complexes, respectively). Perhaps more importantly, all of the cationic complexes decompose rapidly in solution, even at −30 °C, to regenerate mixtures containing the unligated triphosphenium cations **6** or **7**. Therefore, although it is possible to bind cationic triphosphenium ions to these transition metal carbonyl fragments, the products are clearly not as favorable or stable as those formed with the zwitterionic triphosphenium ligand (**1**).

Table 2. Summary of $^{31}P\{^1H\}$ NMR Data for the Complexes of Triphosphenium Tetraphenylborate Salts 6[BPh_4] and 7[BPh_4] with Transition Metal Carbonyls[a]

cation	δP^I	δP^{III}	$^1J_{PP}$	$^1J_{PW}$
6	−235	64	456	
7	−210	23	424	
6–Fe(CO)$_4$	−78	51	411	
7–Fe(CO)$_4$	−54	18	392	
7–Cr(CO)$_5$	−88	27	386	
7–Mo(CO)$_5$	−116	24	373	
7–W(CO)$_5$	−130	22	371	135

[a]Chemical shift values are in parts per million, and coupling constants are in Hertz.

Overall, it appears as if modification of the P(I) system to include a zwitterionic construct is critical in order to access the coordination chemistry of these types of compounds. It is also worth noting that Dillon et al. made the observation that at least one of the flanking tetracoordinate phosphorus atoms needed to bear alkyl substituents or else no products were observed in their study with cationic triphosphenium ions and reactive platinum dimers.[33] While we only looked at cationic triphosphenium ions with aryl substituents, it is worth highlighting that the slight electron-withdrawing nature of the aryl groups on the flanking phosphorus centers in **1** does not prevent it from generating stable and isolable coordination compounds.[34]

X-ray Crystallography. Images of the solid-state structures are shown in Figure 4, important X-ray parameters are listed in Table 3, and metrical parameters are listed in Table 4. The M(CO)$_5$ (M = Cr, Mo, W) complexes (**2M**) are all isomorphic to each other in addition to the corresponding arsenic derivatives,[35] with only negligible differences in torsion angles of the aryl substituents. P–M bond lengths are 2.4599(8), 2.5947(8), and 2.5756(7) Å for Cr, Mo, and W, respectively. These values are on the long side of phosphorus–group 6 metal bonds with a worthwhile comparison being to $Ph_3P\rightarrow$M(CO)$_5$, which possesses phosphorus–metal bond lengths of 2.422(1), 2.560(1), and 2.545(1) Å for Cr, Mo, and W, respectively.[40] P–P bond lengths for **2M** have elongated slightly from the parent ligand, all being within 2.160 and 2.170 Å, consistent with the related decrease in the P–P coupling constants observed in the $^{31}P\{^1H\}$ NMR spectra. This is also characteristic of decreased π-back-bonding from the central phosphorus atom to the flanking phosphorus centers, which would be necessary to observe coordination chemistry. There appears to be no correlation between the P–P coupling constants observed in the $^{31}P\{^1H\}$ NMR spectra and the average bond lengths within these three compounds; the Cr complex has the largest coupling constant and also the longest bond length, where it might be predicted to have the shortest bond lengths on the basis of the $^1J_{P-P}$ couplings. The central phosphorus atom exists in the trigonal pyramidal geometry, consistent with the presence of a second, lone pair of electrons. The CO ligands on each group 6 metal deviate from an ideal octahedral geometry due to the significant steric demands of the ligand framework. There is a slight difference in the M–C bond lengths for the axial (trans to **1**) CO and the equatorial (cis to **1**) CO ligands with the M–C_{ax} bond length being longer in all cases. This is consistent with a small trans effect from ligand **1** as stronger donors typically have a larger effect on the M–C_{ax} bond distance.[40] The structure of **2Fe** is very similar to the group 6 analogues with there being a relatively long P–Fe bond (2.2999(8) Å) and slightly elongated P–P bond lengths compared to **2M** at 2.1826(10) and 2.1822(9) Å, which is again inconsistent with the observed larger coupling constant than the group 6 derivatives. The opposite trend is observed with the M–CO bonds where the M–C_{ax} bond length (1.767(3) Å) is shorter when compared to the M–C_{eq} bond lengths (av. 1.792(3) Å). A typical Fe–P bond length is 2.24–2.27 Å, while extremely bulky phosphines, P(^{t}Bu)$_3$ for example, can extend the Fe–P bond length to 2.37 Å.[41] The phosphorus atom again exists in the AX_3E trigonal pyramidal VSEPR geometry, while the iron center adopts a distorted trigonal bipyramidal AX_5 geometry. The trans CO ligand is bent severely from the ideal 180° with a P–Fe–C bond angle of 159.9(1)°. In all cases, the 6-membered ring exists in a twisted boat conformation, probably due to the considerable steric congestion of the six phenyl groups on the ligand framework. This geometry change from the free ligand is also observed in the analogous arsenic coordination complexes or if {AuCl} is the acceptor (**O**).[34,36] Overall the data obtained from the solid-state structures of **2M** and **2Fe** are consistent with the fact that **1** is a relatively weak σ-donor ligand.

The bimetallic piano-stool complexes **3M** (M = Cr, Mo) are isostructural as evidenced by their similar structure and unit cell parameters. The quality of the models is worse than **2M** in part due to occupational disorder of the M(CO)$_3$ fragment and a dichloromethane solvate, refining to a 68% and 74% occupancy for the M(CO)$_3$ component for the Cr and Mo structures, respectively. Full diagrams and crystallographic tables describing these compounds can be found in the Supporting Information (Figure S25 for Cr; Figure S26 for Mo, Table S-

dx.doi.org/10.1021/ic401766j | Inorg. Chem. 2013, 52, 11438–11449

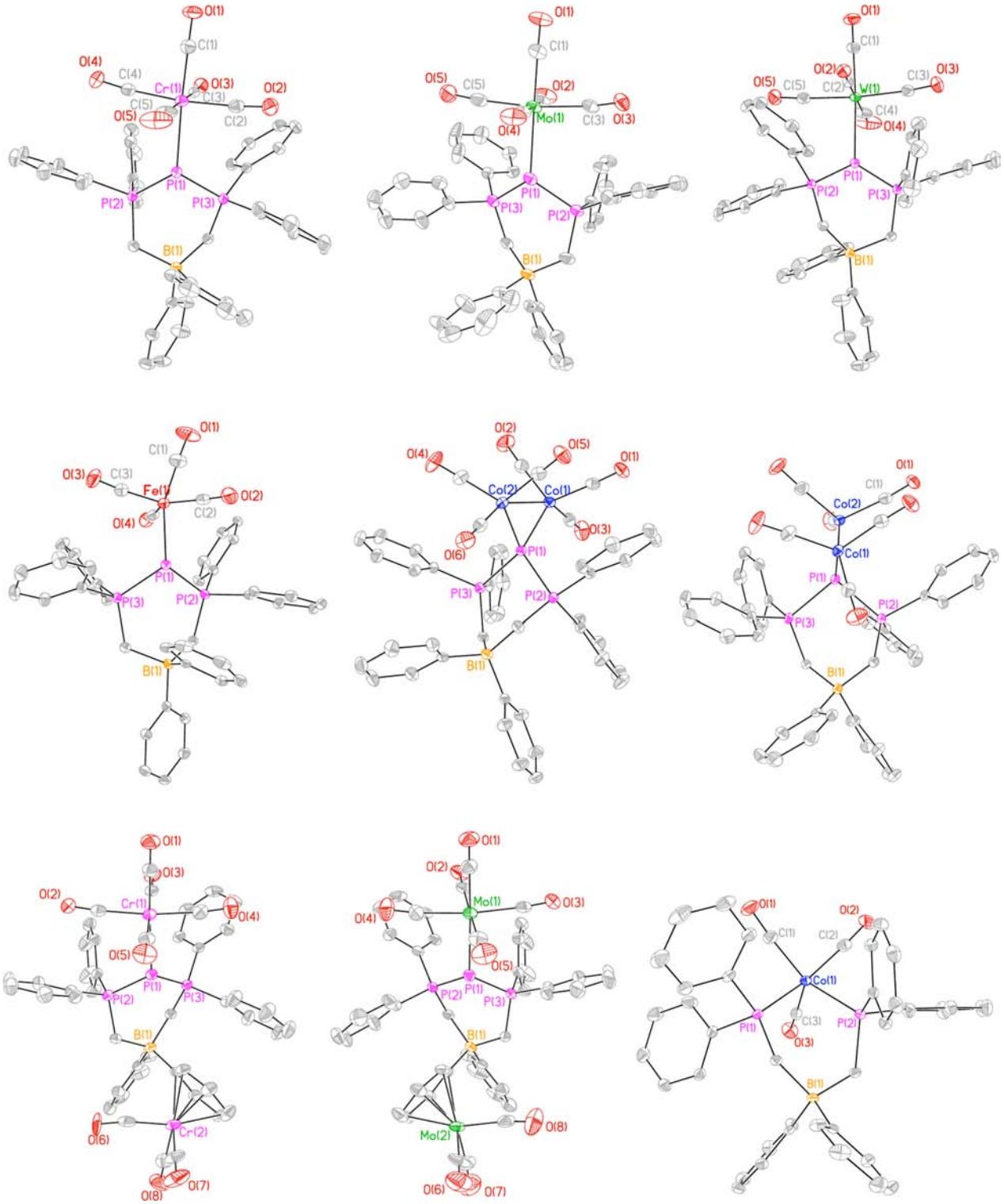

Figure 4. Solid-state structures of the reported compounds. From left to right, top to bottom: **2Cr**, **2Mo**, **2W**, **2Fe**, **4** (two views), **3Cr**, **3Mo**, and **5**. Thermal ellipsoids are drawn at 50% probability, and hydrogen atoms, Et_2O solvates (**2Cr**, **2Fe**, **4**), and occupationally disordered CH_2Cl_2 molecules (**3Cr**, **3Mo**) are removed for clarity.

1). This disorder is observed due to the presence of dichloromethane as a solvent for crystallization, while **2M** crystallizes selectively from a saturated Et_2O solution. In the structure solution of **2M** no residual density above $1.5e^-$ is observed in the Fourier difference map where the second metal center would be expected to be observed. Overall the metrical parameters of **3M** are very comparable with the ones observed in **2M** and warrant no further comment.

The solid-state structure of **4** reveals **1** to be acting as a unique neutral four-electron μ-type ligand. The bonding motif had previously only been observed for triphosphenium ions in the form of a bis-aurinated complex where the substituents on phosphorus had to be isopropyl groups.[34] The complex consists

dx.doi.org/10.1021/ic401766j | *Inorg. Chem.* 2013, 52, 11438−11449

Table 3. Summary of X-ray diffraction Collection and Refinement Details for the Feature Compounds Reported in This Work[a]

	2Cr	2Mo	2W	2Fe	4
formula	$C_{47}H_{44}BCrO_6P_3$, $C_4H_{10}O$	$C_{43}H_{34}BMoO_5P_3$	$C_{43}H_{34}BO_5P_3W$	$C_{42}H_{34}BFeO_4P_3$, $C_4H_{10}O$	$C_{44}H_{34}BCo_2O_6P_3$, $C_4H_{10}O$
fw (g/mol)	860.54	830.36	918.27	836.37	954.41
cryst dimens (mm)	0.173 × 0.084 × 0.073	0.26 × 0.11 × 0.05	0.164 × 0.123 × 0.102	0.110 × 0.090 × 0.084	0.200 × 0.104 × 0.051
crystal color and habit	yellow prism	yellow prism	yellow prism	orange plate	violet prism
crystal system	triclinic	monoclinic	triclinic	orthorhombic	triclinic
space group	$P\bar{1}$	$P2_1/n$	$P\bar{1}$	*Pbcn*	$P\bar{1}$
temp, K	110	110	110	110	110
a, Å	10.024(3)	9.832(4)	10.049(2)	41.905(10)	12.533(4)
b, Å	10.454(4)	18.266(7)	10.488(3)	9.3403(16)	12.565(5)
c, Å	21.700(6)	21.777(8)	21.847(6)	21.160(4)	15.562(6)
α, deg	87.834(5)	90	87.999(8)	90	70.291(13)
β, deg	83.023(5)	98.524(12)	83.125(9)	90	89.234(16)
γ, deg	76.236(6)	90	75.974(9)	90	78.154(14)
V (Å^3)	2192.2(12)	3868(3)	2217.9(10)	8282(3)	2253.8(14)
Z	2	4	2	8	2
F(000)	896	1696	912	3472	984
ρ (g/cm)	1.304	1.426	1.375	1.338	1.406
λ, Å (Mo K*α*)	0.71073	0.71073	0.71073	0.71073	0.71073
μ (cm^{-1})	0.418	0.508	2.752	0.526	0.893
max 2*θ* for data collection, deg	61.02	63.1	66.284	55.82	62.0
measd fraction of data	0.986	0.997	0.982	0.996	0.981
no. of reflns measd	89 497	71 946	87 742	124 931	97 209
no. of unique reflns measd	13 086	12 891	16 470	9869	14 073
R_{merge}	0.0627	0.0521	0.0527	0.1147	0.0544
no. of reflns included in refinement	13 086	12 891	16 470	9869	14 073
no. of params in least squares	525	478	478	507	552
R_1, wR_2	0.0485, 0.1008	0.0406, 0.0831	0.0282, 0.0613	0.0459, 0.0975	0.0387, 0.0788
R_1 (all data), wR_2 (all data)	0.0863, 0.1156	0.0718, 0.0953	0.0354, 0.0632	0.0882, 0.1141	0.0645, 0.0887
GOF	1.035	1.030	1.015	1.009	1.036
min and max peak heights on final Δ*F* map (e$^-$/Å)	−0.531, 0.821	−0.607, 0.711	−0.735, 1.400	−0.743, 0.462	−0.510, 0.511

[a] $R_1 = \Sigma(|F_o| - |F_c|)/\Sigma F_o$, $wR_2 = [\Sigma(w(F_o^2 - F_c^2)^2)/\Sigma(wF_o^4)\ ]^{1/2}$, GOF = $[\ \Sigma(w(F_o^2 - F_c^2)^2)/(\text{no. of reflns} - \text{no. of params})]^{1/2}$.

Table 4. Significant Metrical Parameters and $^{31}P\{^1H\}$ NMR Data for the Reported Compounds[a]

compound	2Cr	2Mo	2W	3Cr	3Mo	2Fe	4
P−M	2.4599(8)	2.5947(8)	2.5756(7)	2.4773(14)	2.5974(13)	2.2999(8)	2.1536(9), 2.1537(9)
P−P	2.1621(9)	2.1626(10)	2.1644(8)	2.1697(16)	2.1737(17)	2.1826(10)	2.1894(8)
	2.1692(9)	2.1604(9)	2.1605(8)	2.1853(14)	2.1583(17)	2.1822(9)	2.2290(8)
P−P−P	95.26(3)	95.99(4)	95.50(3)	94.87(5)	95.17(7)	97.75(3)	97.03
M−C_{ax}	1.856(2)	1.973(2)	1.991(2)	1.852(4)	1.982(5)	1.767(3)	
C_{ax}−O	1.152(3)	1.156(3)	1.150(2)	1.154(4)	1.145(6)	1.156(4)	
M−C_{eq}	1.898(2)	2.062(2)	2.038(2)	1.925(4)	2.065(5)		
	1.905(2)	2.049(2)	2.038(2)	1.918(4)	2.065(6)	1.804(3)	1.799(2), 1.774(2)
	1.897(2)	2.049(2)	2.044(2)	1.904(4)	2.060(6)	1.788(3)	1.785(2), 1.808(2)
	1.905(2)	2.040(2)	2.043(2)	1.916(4)	2.059(6)	1.784(3)	1.765(2), 1.757(2)
C_{eq}−O	1.146(3)	1.134(3)	1.145(2)	1.145(5)	1.140(6)		
	1.142(2)	1.138(3)	1.144(3)	1.154(4)	1.144(6)	1.151(3)	1.145(2), 1.146(2)
	1.149(3)	1.142(3)	1.137(3)	1.149(5)	1.134(7)	1.152(4)	1.143(2), 1.142(2)
	1.145(3)	1.142(3)	1.138(3)	1.144(5)	1.138(7)	1.152(3)	1.146(2), 1.148(2)
Σ°P	332.8	331.7	331.8	335.1	335.3	325.3	346.1, 331.8
M−M							2.6770(8)
δ_P	t −115.8	t −139.4	t −152.0	t −113.7	t −136.2	t −88.6	t 96.8
	d 40.5	d 38.2	d 36.0	d 40.0	d 37.2	d 35.7	d 29.1
$^1J_{P-P}$	364 Hz	350 Hz	345 Hz; $^1J_{^{183}W-P}$ = 134 Hz	365 Hz	353 Hz	378 Hz	257 Hz

[a] Bond lengths are Angstroms, while bond angles are in degrees.

of a staggered $Co_2(CO)_6$ fragment with a Co−Co bond of 2.6770(8) Å. The Co−C bond lengths fall within a range of 1.757(2) and 1.808(2) Å, which is comparable to related systems.[41] P−Co bond lengths are identical at 2.1536(9) and

dx.doi.org/10.1021/ic401766j | *Inorg. Chem.* 2013, 52, 11438−11449

2.1537(9) Å, highlighting the equal donor ability of both lone pairs of electrons on phosphorus. These bonds are longer than the P−Co bond lengths in Cowley's 2,4,6-tri-*tert*-butylphenylphosphinidene $Co_2(CO)_6$ complex (cf. 2.047(6) Å), probably a result of the steric bulk of **1**.[42] P−P bond lengths have expanded when compared to the other coordination complexes of **1** and are significantly different at 2.1894(8) and 2.2290(8) Å. This observation differs from the bis-aurinated complex (**R**) where P−P bond lengths are crystallographically indistinguishable. The phosphorus and two cobalt atoms form a strained triangle with bond angles of 51.57(2)°, 51.57(3)°, and 76.85(3)°, with the later being the Co−P−Co angle. The unique phosphorus atom is formally tetrahedral (AX_4), while the cobalt centers possess a severely distorted trigonal bipyramidal geometry with a CO ligand and the other Co metal center occupying the axial sites (Co−Co−C_{ax} = 153.60(6)° and 156.04(6)°).

CONCLUSIONS

A series of neutral phosphanide metal carbonyl complexes has been prepared and fully characterized. In the case of the group 6 metals, traditional $M(CO)_5$ coordination compounds, **2M**, are produced in high yields, while the analogous $Fe(CO)_4$ complex, **2Fe**, can also be isolated using the same reaction conditions. The molecular geometry and metrical parameters are consistent with **1** being a weak donor ligand with an additional, unused, "lone pair" of electrons on the central phosphorus atom. Simultaneous use of both lone pairs of electrons on phosphorus is observed in **4**, which is produced quantitatively from reaction of $Co_2(CO)_8$ with **1**. This complex represents a rare example of an μ-type 4-electron coordination complex for a neutral phosphorus(I) compound and also possesses a metal−metal bond. Compounds **2M** and **2Fe** are unique zwitterionic triphosphenium metal complexes that cannot be isolated from the analogous charged triphosphenium-based systems. Thus, the anionic borate backbone has a profound influence on the donating ability of the central phosphorus atom, a feature that we look to further exploit in future studies.

EXPERIMENTAL DETAILS

Experimental Methods. All manipulations were performed under inert atmosphere either in a nitrogen-filled MBraun Labmaster 130 Glovebox or on a Schlenk line. Reagents PBr_3 and cyclohexene were obtained from Sigma Aldrich and distilled prior to use, while the group 6 metal carbonyls were also obtained from Sigma Aldrich and sublimed prior to use. Iron pentacarbonyl, diiron nonacarbonyl, and dicobalt octacarboyl were obtained from Alfa Aesar and used as received. The parent phosphanide, **1**,[34] and cationic triphosphenium ions, **6**[Br],[38] **6**[BPh_4],[32] and **7**[BPh_4],[32] were prepared as reported in the literature. Solvents were obtained from Caledon Laboratories and dried using an Innovative Technologies Inc. Solvent Purification System or an MBraun Solvent Purification system. Dried solvents were collected under vacuum and stored under a nitrogen atmosphere in Strauss flasks or in the drybox over 4 Å molecular sieves. Solvents for NMR spectroscopy, $CDCl_3$ and CD_2Cl_2, were stored in the drybox over 4 Å molecular sieves. Solution ^1H, $^{13}C\{^1H\}$, $^{11}B\{^1H\}$, and $^{31}P\{^1H\}$ NMR spectroscopy was recorded on a Varian INOVA 400 MHz spectrometer unless otherwise noted (^1H 400.09 MHz, $^{11}B\{^1H\}$ 128.2 MHz, $^{13}C\{^1H\}$ 100.5 MHz, and $^{31}P\{^1H\}$ 161.82 MHz). All samples for ^1H and $^{13}C\{^1H\}$ NMR spectroscopy were referenced to the residual protons in the deuterated solvent relative to $Si(CH_3)_4$ (CH_2Cl_2 δ_H = 5.32, $^{13}C\{^1H\}$ δ = 54.0; $CDCl_3$ ^1H δ_H = 7.26, $^{13}C\{^1H\}$ δ = 77.1). Chemical shifts for $^{31}P\{^1H\}$ and $^{11}B\{^1H\}$ NMR spectroscopy were referenced to an external standard (85% H_3PO_4; δ_P = 0.0, $BF_3(Et_2O)$; δ_B = 0.0). FT-IR spectroscopy was performed on samples as KBr pellets using a Bruker Tensor 27 FT-IR spectrometer with a resolution of 4 cm^{-1}. FT-Raman spectroscopy was performed on samples flame sealed in glass capillaries using a Bruker RFS 100/S spectrometer with a resolution of 4 cm^{-1}. Mass spectrometry was recorded in house in positive- and negative-ion modes using an electrospray ionization Micromass LCT spectrometer. Melting or decomposition points were determined by flame sealing the sample in capillaries and heating using a Gallenkamp Variable Heater.

X-ray Crystallography. Single-crystal X-ray diffraction studies were performed at the Western University X-ray facility. Crystals were selected under Paratone(N) oil, mounted on a MiTeGen polyimide micromount, and immediately put under a cold stream of nitrogen for data to be collected on a Nonius Kappa-CCD area detector or Bruker Apex II detector using Mo Kα radiation (λ = 0.71073 Å). The Bruker and Nonius instruments operate SMART[43] and COLLECT[44] software, respectively. Unit cell dimensions were determined from a symmetry-constrained fit on the full data set, which was composed of ϕ and ω scans. Frame integration was performed by SAINT;[45] resulting raw data was scaled and absorption corrected using a multiscan averaging of symmetry equivalent data using SADABS.[46] The SHELXTL/PC V6.14 for Windows NT suite of programs was used to solve the structure by direct methods.[47] Subsequent difference Fourier syntheses allowed the remaining atoms to be located, while hydrogen atoms were placed in calculated positions and allowed to ride on the parent atom. In the case of **2Cr**, **2Mo**, **2Fe**, **4**, and **5** all of the non-hydrogen atoms, including Et_2O solvates when necessary, were well ordered and refined with anisotropic thermal parameters. In the case of **3Cr** and **3Mo** the $M(CO)_3$ fragment was occupationally disordered with a dichloromethane molecule in a 68:32 and 74:26 ratio for Cr and Mo, respectively. This model refined suitably, allowing for all atoms in the disordered components to be modeled anisotropically. C−Cl bond lengths in the dichloromethane solvate were restrained to sensible distances using DFIX. For **3Mo**, one chlorine atom on the CH_2Cl_2 solvate shared a position with one of the carbonyl oxygen atoms, while for **3Cr** the best model exists with these two atoms being in close proximity but on separate positions. For **2W** two Et_2O molecules were present in the unit cell (1 per asymmetric unit); however, unlike **2Cr** and **2Fe** this solvate was highly disordered and treated as a diffuse contribution to the overall scattering by SQUEEZE/Platon.[48]

Computational Investigations. Geometry optimizations and frequency calculations were performed using the Compute Canada Shared Hierarchical Academic Research Computing Network (SHARCNET) facilities (www.sharcnet.ca) with the Gaussian09[49] program suites. Geometry optimizations have been calculated using density functional theory (DFT), specifically implementing the M062X method[50] in conjunction with the TZVP basis set[51] for all atoms. Geometry optimizations were not subjected to any symmetry restrictions, and each stationary point was confirmed to be a minimum having zero imaginary vibrational frequencies. Cartesian coordinates for the optimized structures are provided in the Supporting Information. Using these geometries, single-point GIAO NMR calculations including the zeroth-order regular approximation (ZORA) treatment for relativistic effects and spin−orbit coupling[52−56] were conducted using the PW91PW91 method[5758] in conjunction with the all-electron TZ2P basis set using the Amsterdam Density Functional suite of programs (ADF 2013.01).[59−61]

EXPERIMENTAL SECTION

General Synthesis of 2M. To a 3 mL THF solution of **1** 2−3 stoichiometric equivalents of $M(CO)_6$ (M = Cr, Mo, W) in 3 mL of THF were added. The reaction was allowed to stir under UV irradiation for 6 h intervals with the progress being monitored by $^{31}P\{^1H\}$ NMR spectroscopy. The reaction was confirmed to be complete by 100% conversion of the starting material (δ_P = 34 (d), −223 (t) in THF) to the product (δ_P = 40 (d), −116 (t) for Cr, δ_P = 40 (d), −116 (t) for Mo and δ_P = 39 (d), −154 (t) for W, respectively in THF). Volatiles were removed in vacuo to give a yellow/orange

solid, and any excess $M(CO)_6$ was removed by sublimation (50 °C oil bath, −12 °C coldfinger), if necessary. The remaining solid was dissolved in Et_2O (4 mL), and residual solids were removed by filtration. Volatiles of the filtrate were removed in vacuo to give **2M** as a yellow/orange solid.

2Cr. Reagents: **1** (36.0 mg, 0.0606 mmol, 3 mL THF), $Cr(CO)_6$ (40.1 mg, 0.1818 mmol, 3 mL THF). Yield (41.2 mg, 86%); dp = 174−177 °C powder turns black. ^{1}H NMR (400 MHz $CDCl_3$): 2.28 (dd, 4H, $^2J_{P-H}$ = 15.2 Hz, $^3J_{P-H}$ = 3.2 Hz), 6.82 (t, 2H, $^3J_{H-H}$ = 6.8 Hz), 6.88 (t, 4H, $^3J_{H-H}$ = 7.2 Hz), 7.03 (d, 4H, $^3J_{H-H}$ = 7.6 Hz), 7.34 (td, 8H, $^3J_{H-H}$ = 7.8 Hz, $^3J_{P-H}$ = 2.8 Hz), 7.42−7.53 (overlapping multiplet; 12H). $^{31}P\{^1H\}$ NMR (161.8 MHz $CDCl_3$): −116 (t, 1P, $^1J_{P-P}$ = 363.9 Hz), 40.5 (d, 2P, $^1J_{P-P}$ = 363.9 Hz). $^{11}B\{^1H\}$ (128.3 MHz $CDCl_3$): −14.8. $^{13}C\{^1H\}$ NMR (100.5 MHz $CDCl_3$): 20.0−22.0 (br), 123.7, 126.8, 128.6 (dd, $^1J_{P-C}$ = 68.1 Hz, $^2J_{P-C}$ = 4.4 Hz), 129.2 (d, $^2J_{P-C}$ = 6.3 Hz), 132.47, 132.53, 132.8 (dd, $^2J_{P-C}$ = 10.1 Hz, $^3J_{P-C}$ = 4.4 Hz), 158−160 (br), 215.7 (t, $^2J_{P-C}$ = 3.4 Hz), 221.8 (d, $^2J_{P-C}$ = 2.5 Hz). FT-IR (cm^{-1} (ranked intensity)): 447 (13), 526 (10), 648 (4), 690 (7), 735 (6), 849 (11), 874 (12), 909 (14), 1099 (8), 1435 (9), 1586 (15), 1900 (2), 1939 (1), 1986 (5), 2058 (3). FT-Raman (cm^{-1} (ranked intensity)): 104 (2), 222 (11), 390 (7), 483 (10), 618 (15), 1000 (1), 1029 (6), 1101 (13), 1890 (9), 1908 (12), 1979 (3), 2060 (8), 2888 (14), 3060 (5). HRMS calcd for $C_{43}H_{34}B_1Cr_1Na_1O_5P_3$ ([M + Na]$^+$) 809.10235 *m/z*, found 809.10459 *m/z*. Anal. Found (Calcd) for $C_{43}H_{34}B_1Cr_1O_5P_3$: C, 65.36 (65.60); H, 4.54 (4.36).

2Mo. Reagents: **1** (33.0 mg, 0.0555 mmol, 3 mL THF), $Mo(CO)_6$ (29.3 mg, 0.1110 mmol, 3 mL THF). Yield (38.2 mg, 83%); dp =182−184 °C powder turns black. ^{1}H NMR (400 MHz $CDCl_3$): 2.26 (dd, 4H, $^2J_{P-H}$ = 15.2 Hz, $^3J_{P-H}$ = 3.6 Hz), 6.82 (t, 2H, $^3J_{H-H}$ = 6.8 Hz), 6.89 (t, 4H, $^3J_{H-H}$ = 7.4 Hz), 7.04 (d, 4H, $^3J_{H-H}$ = 7.6 Hz), 7.36 (td, 8H, $^3J_{H-H}$ = 7.8 Hz, $^3J_{P-H}$ = 3.2 Hz), 7.42−7.53 (overlapping multiplet; 12H). $^{31}P\{^1H\}$ NMR (161.8 MHz $CDCl_3$): −139 (t, 1P, $^1J_{P-P}$ = 350.6 Hz), 38 (d, 2P, $^1J_{P-P}$ = 350.6 Hz). $^{11}B\{^1H\}$ (128.3 MHz $CDCl_3$): −14.6. $^{13}C\{^1H\}$ NMR (100.5 MHz $CDCl_3$): 19.0−22.0 (br), 123.6, 126.7, 128.9 (dd, $^1J_{P-C}$ = 68.1 Hz, $^2J_{P-C}$ = 4.4 Hz), 129.1 (d, $^2J_{P-C}$ = 9.6 Hz), 132.3, 132.5, 132.6 (dd, $^2J_{P-C}$ = 10.2 Hz, $^3J_{P-C}$ = 4.2 Hz), 158−160 (br), 204.5 (broad triplet), 210.2 (d, $^2J_{P-C}$ = 2.8 Hz). FT-IR (cm^{-1} (ranked intensity)): 476 (15), 499 (13), 526 (9), 553 (14), 585 (7), 604 (6), 670 (4), 735 (8), 849 (12), 1101 (11), 1436 (10), 1901 (2), 1944 (1), 1993 (5), 2069 (3). FT-Raman (cm^{-1} (ranked intensity)): 100 (3), 214 (12), 224 (11), 406 (10), 456 (9), 999 (2), 1028 (8), 1104 (14), 1586 (6), 1887 (4), 1955 (15), 1985 (1), 2069 (7), 3061 (5). HRMS calcd for $C_{43}H_{34}B_1Mo_1Na_1O_5P_3$ ([M + Na]$^+$) 855.06798 *m/z*, found 855.06441 *m/z*. Anal. Found (Calcd) for $C_{43}H_{34}B_1Mo_1O_5P_3$: C, 62.18 (62.19); H, 4.11 (4.13).

2W. Reagents: **1** (96.0 mg, 0.1616 mmol, 3 mL THF), $W(CO)_6$ (113.7 mg, 0.3232 mmol, 3 mL THF). Yield (130 mg, 88%); dp =202−205 °C powder turns gray. ^{1}H NMR (400 MHz $CDCl_3$): 2.29 (dd, 4H, $^2J_{P-H}$ = 15.2 Hz, $^3J_{P-H}$ = 4.0 Hz), 6.82 (t, 2H, $^3J_{H-H}$ = 6.8 Hz), 6.89 (t, 4H, $^3J_{H-H}$ = 7.4 Hz), 7.04 (d, 4H, $^3J_{H-H}$ = 7.6 Hz), 7.36 (td, 8H, $^3J_{H-H}$ = 7.8 Hz, $^3J_{P-H}$ = 3.2 Hz), 7.44 (d, 4H, $^3J_{H-H}$ = 7.8 Hz), 7.46 (d, 2H, $^3J_{H-H}$ = 7.8 Hz), 7.53 (tq; 4H, $^3J_{H-H}$ = 7.8 Hz, $^3J_{P-H}$ = 3.2 Hz). $^{31}P\{^1H\}$ NMR (161.8 MHz $CDCl_3$): −152 (t, 1P, $^1J_{P-P}$ = 345.4 Hz, $^1J_{W-P}$ = 134.1 Hz), 36 (d, 2P, $^1J_{P-P}$ = 345.4 Hz). $^{11}B\{^1H\}$ (128.3 MHz $CDCl_3$): −14.5. $^{13}C\{^1H\}$ NMR (100.5 MHz $CDCl_3$): 19.0−21.0 (br), 123.7, 126.7, 128.5 (dd, $^1J_{P-C}$ = 67.3 Hz, $^2J_{P-C}$ = 5.0 Hz), 129.2 (d, $^2J_{P-C}$ = 11.0 Hz), 132.4 ($^4J_{P-C}$ = 2.1 Hz), 132.5, 132.7 (dd, $^2J_{P-C}$ = 10.3 Hz, $^3J_{P-C}$ = 4.2 Hz), 158−160 (br), 196.2 (t, $^3J_{P-C}$ = 3.1 Hz), 198.3 (d, $^2J_{P-C}$ = 18.1 Hz). FT-IR (cm^{-1} (ranked intensity)): 459 (13), 527 (8), 578 (6), 594 (5), 690 (7), 735 (9), 849 (12), 1103 (11), 1436 (10), 1898 (2), 1935 (1), 1984 (3), 2067 (4), 3039 (14), 3061 (15). FT-Raman (cm^{-1} (ranked intensity)): 108 (1), 224 (15), 433 (2), 471 (8), 617 (14), 999 (4), 1028 (11), 1104 (13), 1586 (6), 1882 (5), 1956 (10), 1975 (3), 2067 (9), 2893 (12), 3061 (7). HRMS calcd for $C_{43}H_{34}BNaO_5P_3W_1$ ([M + Na]$^+$) 941.11322 *m/z*, found 941.11298 *m/z*. Anal. Found (Calcd) for $C_{43}H_{34}BO_5P_3W_1$: C, 56.25 (56.21); H, 3.71 (3.73).

Synthesis of 2Fe. To a 5 mL THF solution of **1** 3 stoichiometric equivalents of $Fe(CO)_5$ were added. The reaction was allowed to stir under UV irradiation for 6 h intervals with the progress being monitored by $^{31}P\{^1H\}$ NMR spectroscopy. The reaction was confirmed to be complete by 100% conversion of the starting material (δ_P = 34 (d), −223 (t) in THF) to the product (δ_P = 37, −90 in THF). Volatiles were removed in vacuo to give a orange solid, and any excess $M(CO)_5$ was also removed in vacuo. Remaining solid was dissolved in Et_2O (4 mL), and residual solids were removed by filtration. Volatiles of the filtrate were removed in vacuo to give **2Fe** as an orange solid.

Reagents: **1** (60.2 mg, 0.101 mmol, 5 mL THF), $Fe(CO)_5$ (59.0 mg, 41.0 μL 0.303 mmol). Yield (67.8 mg, 88%); dp =154−156 °C powder turns black. ^{1}H NMR (400 MHz $CDCl_3$): 2.39 (d, 4H, $^2J_{P-H}$ = 16.0 Hz), 6.83 (t, 2H, $^3J_{H-H}$ = 7.2 Hz), 6.92 (t, 4H, $^3J_{H-H}$ = 7.0 Hz), 7.08 (d, 4H, $^3J_{H-H}$ = 7.4 Hz), 7.35 (td, 8H, $^3J_{H-H}$ = 7.8 Hz, $^3J_{P-H}$ = 2.8 Hz), 7.44−7.54 (m, 10H). $^{31}P\{^1H\}$ NMR (161.8 MHz $CDCl_3$): −88.6 (t, 1P, $^1J_{P-P}$ = 378.2 Hz), 35.7 (d, 2P, $^1J_{P-P}$ = 378.2 Hz). $^{11}B\{^1H\}$ (128.3 MHz $CDCl_3$): −14.4.$^{13}C\{^1H\}$ NMR (100.5 MHz $CDCl_3$): 19.0−21.0 (br), 123.6, 126.7, 128.2 (dd, $^1J_{P-C}$ = 56.8 Hz, $^2J_{P-C}$ = 4.2 Hz), 128.8 (d, $^2J_{P-C}$ = 12.2 Hz), 132.1, 132.3, 132.7−132.9 (m), 215.7 (br t). FT-IR (cm^{-1} (ranked intensity)): 468 (14), 513 (13), 619 (10), 686 (7), 734 (9), 801 (1), 1022 (3), 1096 (2), 1262 (4), 1435 (12), 1483 (15), 1927 (5), 1960 (6), 2036 (8), 2964 (11). FT-Raman (cm^{-1} (ranked intensity)): 109 (2), 222 (8), 262 (13), 442 (9), 491 (14), 617 (11), 1000 (1), 1029 (4), 1586 (3), 1939 (7), 1955 (6), 1970 (15), 2906 (12), 3056 (5). ESI-MS: 761.2 *m/z* ($C_{42}H_{33}B_1Fe_1O_4P_3$; [M − H$^-$]$^+$).

Synthesis of 4. To a dark blue solution of $Co_2(CO)_8$ in CH_2Cl_2 was added 1 stoichiometric equivalent of **1** in CH_2Cl_2 over the course of 4 min. During addition the reaction mixture gradually turned an intense purple color with no further color change observed within 5 min of **1** being completely added. Analysis of the reaction mixture by $^{31}P\{^1H\}$ NMR spectroscopy confirmed the reaction to be complete, after which volatiles were removed in vacuo to give **4** as a dark purple powder.

Reagents: **1** (103.0 mg, 0.1734 mmol, 3 mL CH_2Cl_2), $Co_2(CO)_8$ (59.3 mg, 0.1734 mmol, 3 mL CH_2Cl_2). Yield (152 mg, 99%); dp =153−156 °C. ^{1}H NMR (600 MHz $CDCl_3$): 2.71 (dd, 4H, $^2J_{P-H}$ = 15.6 Hz, $^3J_{P-H}$ = 3.0 Hz), 6.75 (t, 2H, $^3J_{H-H}$ = 7.2 Hz), 6.80 (t, 4H, $^3J_{H-H}$ = 7.2 Hz), 6.92 (d, 4H, $^3J_{H-H}$ = 6.8 Hz), 7.30 (t, 8H, $^3J_{H-H}$ = 7.2 Hz), 7.47 (t; 4H, $^3J_{H-H}$ = 7.2 Hz), 7.53, (q, 8H, $^3J_{H-H}$ = 6.8 Hz). $^{31}P\{^1H\}$ NMR (161.8 MHz $CDCl_3$): 29 (d, 2P, $^1J_{P-P}$ = 257.3 Hz), 97 (t, 1P, $^1J_{P-P}$ = 257.3 Hz). $^{11}B\{^1H\}$ (128.3 MHz $CDCl_3$): −14.6. $^{13}C\{^1H\}$ NMR (100.5 MHz $CDCl_3$): 15.0−17.0 (br), 123.4, 125.6 (dd, $^1J_{P-C}$ = 34.9 Hz, $^2J_{P-C}$ = 4.0 Hz), 127.0, 128.7 (t, $^3J_{P-C}$ = 5.8 Hz), 131.2, 133.0, 133.4 (t, $^2J_{P-C}$ = 3.8 Hz), 157.0−159.0 (br), 205.5. FT-IR (cm^{-1} (ranked intensity)): 465 (12), 516 (10), 546 (8), 688 (5), 700 (7), 717 (15), 738 (6), 860 (13), 1055 (14), 1101 (9), 1943 (4), 1972 (2), 1999 (1), 2044 (3). FT-Raman (cm^{-1} (ranked intensity)): 186 (2), 341 (15), 443 (13), 1000 (1), 1030 (9), 1100 (11), 1587 (5), 1939 (8), 1949 (3), 1960 (6), 1969 (4), 1984 (10), 2042 (14) 2883 (12), 3057 (7). ESI-MS: 903.0 *m/z*, $C_{44}H_{34}BCo_2NaO_6P_3$ ([M + Na]$^+$), 875.0 *m/z* ([M + Na − CO]$^+$), 847.0 *m/z* ([M + Na − 2CO]$^+$), 819.0 *m/z* ([M + Na − 3CO]$^+$), 791.0 *m/z* ([M + Na - 4CO]$^+$), 763.0 *m/z* ([M + Na − 5CO]$^+$), 735.1 *m/z* ([M + Na − 6CO]$^+$). HRMS calcd for $C_{44}H_{34}B_1Co_2Na_1O_6P_3$ ([M + Na]$^+$) 903.02304 *m/z*, found 903.02260 *m/z*. Anal. Found (calcd) for $C_{44}H_{34}Co_2B_1O_6P_3$: C, 58.13 (60.03); H, 3.75 (3.89).

Reactions That Produced Minor Quantities of 3M. To a THF solution of **1** 5−10 stoichiometric equivalents of $M(CO)_6$ (M = Cr, Mo, W) were added, and the mixture was irradiated with UV light for 3 days. Small amounts of **3M** could be observed in the $^{31}P\{^1H\}$ NMR spectrum, typically in approximately 10% yield compared to the **2M** product (see Figures S21, S22, and S23, Supporting Information, for $^{31}P\{^1H\}$ NMR of the Cr, Mo, and W derivatives, respectively). Prolonged irradiation or a larger excess of $M(CO)_6$ have so far been unsuccessful in forcing the reaction to proceed to form **3M** exclusively.

Reactions of 6[Br] with $M(CO)_6$. To a solution of **6**[Br] in 3 mL of CH_3CN were added 3 stoichiometric equivalents of $M(CO)_6$ (M = Cr, Mo, W) in 3 mL of THF. The reaction mixture was irradiated for UV light for 3 days and monitored by $^{31}P\{^1H\}$ NMR spectroscopy

dx.doi.org/10.1021/ic401766j | Inorg. Chem. 2013, 52, 11438−11449

several times every 24 h. No signs of product formation were observed in the $^{31}P\{^{1}H\}$ NMR spectrum, even though the reaction mixture had turned the characteristic bright yellow color. In the case of $Cr(CO)_6$ noticeable decomposition was observed in the vial and in the $^{31}P\{^{1}H\}$ NMR spectrum after 48 h.

Reactions of 7[BPh_4] with (THF)M$(CO)_5$. A solution containing 2 stoichiometric equivalents of $M(CO)_6$ (M = Cr, Mo, W) in THF was irradiated for 1 h, sparged with N_2 for 15 min, and then added to a solution of **7**[Br] in THF. Reaction mixtures were stirred overnight; then all volatile components were removed under reduced pressure. Analysis of the resultant solids using $^{31}P\{^{1}H\}$ NMR spectroscopy revealed the presence of both complexed and free triphosphenium cations in all cases; specific chemical shift data are listed in Table 2. The unstable nature of the resultant complexes in solution even at low temperature precluded efforts for separation and isolation.

Reactions of 6[BPh_4] or 7[BPh_4] with $Fe_2(CO)_9$. A red solution containing 2 stoichiometric equivalents of $Fe_2(CO)_9$ in THF was added to a colorless solution of **6**[BPh_4] or **7**[BPh_4] in THF. Reaction mixtures were stirred overnight; then all volatile components were removed under reduced pressure. Analysis of the resultant materials using $^{31}P\{^{1}H\}$ NMR spectroscopy indicated the presence of both complexed and free triphosphenium cations in both cases; again, specific chemical shift data are listed in Table 2. The mixtures again proved to be intractable and prevented purification and isolation.

■ ASSOCIATED CONTENT

Ⓢ Supporting Information

Complete NMR spectral data, selected ESI-MS data, stacked NMR spectra highlighting the presence of the piano-stool compounds, and full diagrams of the solid-state structures depicting the disordered CH_2Cl_2 in **3M**, and Cartesian coordinates for calculated structures. This material is available free of charge via the Internet at http://pubs.acs.org.

■ AUTHOR INFORMATION

Corresponding Author

*E-mail: pragogna@uwo.ca.

Notes

The authors declare no competing financial interest.

■ ACKNOWLEDGMENTS

We thank the Natural Science and Engineering Research Council of Canada (NSERC), the Ontario Government, the Canadian Foundation of Innovation (CFI), The University of Western Ontario, and The University of Windsor for their generous funding.

■ REFERENCES

(1) Lammertsma, K. *Top. Curr. Chem.* **2003**, *237*, 95.
(2) Cowley, A. H. *Acc. Chem. Res.* **1997**, *30*, 445.
(3) Cowley, A. H.; Barron, A. R. *Acc. Chem. Res.* **1988**, *21*, 81.
(4) Stephan, D. W. *Angew. Chem., Int. Ed.* **2000**, *39*, 314.
(5) Weber, L. *Eur. J. Inorg. Chem.* **2007**, 4095.
(6) Mathey, F. *Dalton Trans.* **2007**, 1861.
(7) Marinetti, A.; Mathey, F.; Fischer, J.; Mitschler, A. *J. Am. Chem. Soc.* **1982**, *104*, 4484.
(8) Hitchcock, P. B.; Lappert, M. F.; Leung, W.-P. *J. Chem. Soc., Chem. Commun.* **1987**, 1282.
(9) Lammertsma, K.; Vlaar, M. J. M. *J. Org. Chem.* **2002**, 1127.
(10) Mathey, F.; Tran Huy, N. H.; Marinetti, A. *Helv. Chim. Acta* **2001**, *84*, 2938.
(11) Aktaş, H.; Slootweg, J. C.; Lammertsma, K. *Angew. Chem., Int. Ed.* **2010**, *49*, 2102.
(12) Ehlers, A. W.; Baerends, E. J.; Lammertsma, K. *J. Am. Chem. Soc.* **2002**, *124*, 2831.
(13) Schulten, C.; Frantzius, G. v.; Schnakenburg, G.; Espinosa, A.; Streubel, R. *Chem. Sci.* **2012**, *3*, 3526.
(14) Duffy, M. P.; Ting, L. Y.; Nicholls, L.; Li, Y.; Ganguly, R.; Mathey, F. *Organometallics* **2012**, *31*, 2936.
(15) Arduengo, A. J.; Carmalt, C. J.; Clyburne, J. A. C.; Cowley, A. H.; Pyatib, R. *Chem. Commun.* **1997**, 981.
(16) Alcarazo, M.; Radkowski, K.; Mehler, G.; Goddard, R.; Furstner, A. *Chem. Commun.* **2013**, *49*, 3140.
(17) Back, O.; Henry-Ellinger, M.; Martin, C. D.; Martin, D.; Bertrand, G. *Angew. Chem., Int. Ed.* **2013**, *52*, 2939.
(18) Protasiewicz, J. D. *Eur. J. Inorg. Chem.* **2012**, *29*, 4539.
(19) Partyka, D. V.; Washington, M. P.; Updegraff, J. B., III; Woloszynek, R. A.; Protasiewicz, J. D. *Angew. Chem., Int. Ed.* **2008**, *47*, 7489.
(20) Surgenor, B. A.; Buhl, M.; Slawin, A. M.; Woollins, J. D.; Kilian, P. *Angew. Chem., Int. Ed.* **2012**, *51*, 10150.
(21) Henn, J.; Meindl, K.; Oechsner, A.; Schwab, G.; Koritsanszky, T.; Stalke, D. *Angew. Chem., Int. Ed.* **2010**, *49*, 2422.
(22) Stalke, D. *Chem.—Eur. J.* **2011**, *17*, 9264.
(23) Stey, T.; Henn, J.; Stalke, D. *Chem. Commun.* **2007**, 413.
(24) Stey, T.; Pfeiffer, M.; Henn, J.; Pandey, S. K.; Stalke, D. *Chem.—Eur. J.* **2007**, *13*, 3636.
(25) Schmidpeter, A. *Angew. Chem., Int. Ed. Engl.* **1982**, *21*, 63.
(26) Schmidpeter, A.; Lochschmidt, S.; Karaghiosoff, K.; Sheldrick, W. S. *J. Chem. Soc., Chem. Commun.* **1985**, 1447.
(27) Schmidpeter, A.; Lochschmidt, S.; Sheldrick, W. S. *Angew. Chem., Int. Ed.* **1982**, *21*, 63.
(28) Schmidpeter, A.; Lochschmidt, S.; Sheldrick, W. S. *Angew. Chem., Int. Ed.* **1985**, *24*, 226.
(29) Ellis, B. D.; Macdonald, C. L. B. *Coord. Chem. Rev.* **2007**, *251*, 936.
(30) Coffer, P. K.; Dillon, K. B. *Coord. Chem. Rev.* **2013**, *257*, 910.
(31) Ellis, B. D.; Dyker, C. A.; Decken, A.; Macdonald, C. L. B. *Chem. Commun.* **2005**, 1965.
(32) Ellis, B. D.; Macdonald, C. L. B. *Inorg. Chem.* **2006**, *45*, 6864.
(33) Coffer, P. K.; Deng, R. M. K.; Dillon, K. B.; Fox, M. A.; Olivey, R. J. *Inorg. Chem.* **2012**, *51*, 9799.
(34) Dube, J. W.; Macdonald, C. L. B.; Ragogna, P. J. *Angew. Chem., Int. Ed* **2012**, *51*, 13026.
(35) Dube, J. W.; Ragogna, P. J. *Chem.—Eur. J.* **2013**, *19*, 11768.
(36) Grim, S. O.; McAllister, P. R.; Singer, R. M. *Chem. Commun.* **1969**, 38.
(37) Ellis, B. D.; Macdonald, C. L. B. *Inorg. Chem.* **2004**, *43*, 5981.
(38) Norton, E. L.; Szekely, K. L. S.; Dube, J. W.; Bomben, P. G.; Macdonald, C. L. B. *Inorg. Chem.* **2008**, *47*, 1196.
(39) Whyte, T.; Williams, G. A. *Aust. J. Chem.* **1995**, *48*, 1045.
(40) Aroney, M. J.; Buys, I. E.; Davies, M. S.; Hambley, T. W. *J. Chem. Soc., Dalton Trans.* **1994**, 2828.
(41) Howell, J. A. S.; Palin, M. G.; McArdle, P.; Cunningham, D.; Goldschmidt, Z.; Gottlieb, H. E.; Hezroni-Langerman, D. *Inorg. Chem.* **1993**, *32*, 3493.
(42) Arif, A. M.; Cowley, A. H.; Norman, N. C.; Orpen, A. G.; Pakulski, M. *Organometallics* **1988**, *7*, 309.
(43) *SMART*; Bruker AXS Inc.: Madison, WI, 2001.
(44) *COLLECT*; Nonius BV: Delft, The Netherlands, 2001.
(45) *SAINT*; Bruker AXS Inc., Madison, Wisconsin, USA, 2007.
(46) *SADABS*; Bruker AXS Inc.: Madison, WI, 2001.
(47) Sheldrick, G. M. *Acta Crystallogr., Sect. A: Found Crystallogr.* **2008**, *64*, 112.
(48) PLATON; Spek, A. L. *Acta Crystallogr.* **2009**, *D65*, 148.
(49) Frisch, M. J.; Trucks, G. W.; Schlegel, H. B.; Scuseria, G. E.; Robb, M. A.; Cheeseman, J. R.; Scalmani, G.; Barone, V.; Mennucci, B.; Petersson, G. A.; Nakatsuji, H.; Caricato, M.; Li, X.; Hratchian, H. P.; Izmaylov, A. F.; Bloino, J.; Zheng, G.; Sonnenberg, J. L.; Hada, M.; Ehara, M.; Toyota, K.; Fukuda, R.; Hasegawa, J.; Ishida, M.; Nakajima, T.; Honda, Y.; Kitao, O.; Nakai, H.; Vreven, T.; Montgomery, J., J. A.; Peralta, J. E.; Ogliaro, F.; Bearpark, M.; Heyd, J. J.; Brothers, E.; Kudin, K. N.; Staroverov, V. N.; Kobayashi, R.; Normand, J.; Raghavachari, K.; Rendell, A.; Burant, J. C.; Iyengar, S. S.; Tomasi, J.; Cossi, M.; Rega,

N.; Millam, N. J.; Klene, M.; Knox, J. E.; Cross, J. B.; Bakken, V.; Adamo, C.; Jaramillo, J.; Gomperts, R.; Stratmann, R. E.; Yazyev, O.; Austin, A. J.; Cammi, R.; Pomelli, C.; Ochterski, J. W.; Martin, R. L.; Morokuma, K.; Zakrzewski, V. G.; Voth, G. A.; Salvador, P.; Dannenberg, J. J.; Dapprich, S.; Daniels, A. D.; Farkas, Ö.; Foresman, J. B.; Ortiz, J. V.; Cioslowski, J.; Fox, D. J. *Gaussian09*, Revision C012009; Gaussian, Inc.: Wallingford, CT, 2009.

(50) Zhao, Y.; Truhlar, D. G. *Theor. Chem. Acc.* **2008**, *120*, 215.

(51) Schafer, A.; Huber, C.; Ahlrichs, R. *J. Chem. Phys.* **1994**, *100*, 5829.

(52) Schreckenbach, G.; Ziegler, T. *J. Phys. Chem.* **1995**, *99*, 606.

(53) Schreckenbach, G.; Ziegler, T. *Int. J. Quantum Chem.* **1997**, *61*, 899.

(54) Schreckenbach, G.; Ziegler, T. *Theor. Chem. Acc.* **1998**, *99*, 71.

(55) Wolff, S. K.; Ziegler, T. *J. Chem. Phys.* **1998**, *109*, 895.

(56) Wolff, S. K.; Ziegler, T.; van Lenthe, E.; Baerends, E. J. *J. Chem. Phys.* **1999**, *110*, 7689.

(57) Perdew, J. P.; Burke, K.; Wang, Y. *Phys. Rev. B* **1996**, *54*, 16533.

(58) Perdew, J. P.; Chevary, J. A.; Vosko, S. H.; Jackson, K. A.; Pederson, M. R.; Singh, D. J.; Fiolhais, C. *Phys. Rev. B* **1992**, *46*, 6671.

(59) Guerra, C. F.; Snijders, J. G.; te Velde, G.; Baerends, E. J. *Theor. Chem. Acc.* **1998**, *99*, 391.

(60) te Velde, G.; Bickelhaupt, F. M.; Baerends, E. J.; Guerra, C. F.; Van Gisbergen, S. J. A.; Snijders, J. G.; Ziegler, T. *J. Comput. Chem.* **2001**, *22*, 931.

(61) *ADF2013,01*; SCM, Theoretical Chemistry, Vrije Universiteit: The Netherlands, 2013.